The Astronomical Journal, 152:195 (12pp), 2016 December doi:10.3847/0004-6256/152/6/195

THE SHORT ROTATION PERIOD OF HI'IAKA, HAUMEA'S LARGEST SATELLITE

Danielle M. Hastings[1,2], Darin Ragozzine[2,3], Daniel C. Fabrycky[4], Luke D. Burkhart[5,6], Cesar Fuentes[7], Jean-Luc Margot[1], Michael E. Brown[8], and Matthew Holman[5]
[1] University of California, Los Angeles, Department of Earth, Planetary, and Space Sciences, 595 Charles Young Drive East, Los Angeles, CA 90095, USA; dhastings@g.ucla.edu
[2] Florida Institute of Technology, Department of Physics and Space Sciences, 150 West University Boulevard, Melbourne, FL 32901, USA
[3] Brigham Young University, BYU Department of Physics and Astronomy N283 ESC, Provo, UT 84602, USA
[4] Department of Astronomy and Astrophysics, University of Chicago, 5640 South Ellis Avenue, Chicago, IL 60637, USA
[5] Harvard-Smithsonian Center for Astrophysics, 60 Garden Street, Cambridge, MA 02138, USA
[6] Yale University, Department of Physics, 217 Prospect Street, New Haven, CT 06511, USA
[7] Departamento de Astronomía, Universidad de Chile, Camino El Observatorio 1515, Santiago, Chile
[8] California Institute of Technology, Division of Geological and Planetary Sciences, MC 150-21, Pasadena, CA 91125, USA
Received 2016 August 12; revised 2016 September 28; accepted 2016 September 29; published 2016 November 29

ABSTRACT

Hi'iaka is the larger outer satellite of the dwarf planet Haumea. Using relative photometry from the *Hubble Space Telescope* and Magellan and a phase dispersion minimization analysis, we have identified the rotation period of Hi'iaka to be ~9.8 hr (double peaked). This is ~120 times faster than its orbital period, creating new questions about the formation of this system and possible tidal evolution. The rapid rotation suggests that Hi'iaka could have a significant obliquity and spin precession that could be visible in light curves within a few years. We then turn to an investigation of what we learn about the (currently unclear) formation of the Haumea system and family based on this unexpectedly rapid rotation rate. We explore the importance of the initial semimajor axis and rotation period in tidal evolution theory and find that they strongly influence the time required to despin to synchronous rotation, relevant to understanding a wide variety of satellite and binary systems. We find that despinning tides do not necessarily lead to synchronous spin periods for Hi'iaka, even if it formed near the Roche limit. Therefore, the short rotation period of Hi'iaka does not rule out significant tidal evolution. Hi'iaka's spin period is also consistent with formation near its current location and spin-up due to Haumea-centric impactors.

Key words: Kuiper belt objects: individual (Haumea) – planets and satellites: dynamical evolution and stability – planets and satellites: individual (Hi'iaka) – techniques: photometric

Supporting material: machine-readable table

1. INTRODUCTION

The dwarf planet Haumea stands out from the rest of its Kuiper Belt counterparts. It has the shortest known rotation period ($P_{\rm rot} = 3.9154$ hr) of objects its size (Rabinowitz et al. 2006). Haumea is also known to have two regular satellites, Hi'iaka and Namaka (Ragozzine & Brown 2009), and a collisional family of smaller objects associated with it (Brown et al. 2007). These family members share many unusual properties with Haumea, including strong water ice spectra (Schaller & Brown 2008; Trujillo et al. 2011; Carry et al. 2012), high albedos (Elliot et al. 2010), and possibly a more rapid mean rotational period of 6.27 ± 1.19 hr compared to a mean rotational period of 7.65 ± 0.54 hr (Thirouin et al. 2016) for other Kuiper Belt objects (KBOs), in addition to their dynamically clustered orbits (Marcus et al. 2011; Lykawka et al. 2012; Volk & Malhotra 2012). All of these properties point to formation by a major collision that can impart rapid spin to Haumea and generate the satellites and family.

Existing formation hypotheses cannot self-consistently explain all the properties of Haumea's formation (Ortiz et al. 2012; Campo-Bagatin et al. 2016). For example, models that invoke a slow impactor to keep the Haumea family very tightly clustered (Leinhardt et al. 2010) are improbable (Levison et al. 2008; Campo-Bagatin et al. 2016). These mechanisms might be reconciled if Haumea and possibly other large KBOs were near-equal-size binaries that were eventually destabilized, potentially due to three-body dynamical effects of the Sun (Marcus et al. 2011; Brown et al. 2012; Porter & Grundy 2012). Though this can create a slow impactor without relying on a low-probability heliocentric impact, whether it is more plausible than other hypotheses requires further study.

One avenue for improving our understanding of the formation of Haumea is to study its two moons. Their nearly circular and coplanar orbits suggest that they formed as a direct consequence of the same event that spun up Haumea (though it is not impossible that this was a different event from the formation of the family; Schlichting & Sari 2009). Therefore, their physical and orbital properties may contain important clues.

Hi'iaka and Namaka have nominal masses of ~0.5% and ~0.05% of Haumea's mass ($M_{\rm H}$), where $M_{\rm H} = (4.006 \pm 0.040) \times 10^{21}$ kg, and nominal radii of 150 and 75 km, respectively (Ragozzine & Brown 2009). Due to uncertainties in density and brightness measurements, these values may have uncertainties on the level of tens of percent. The satellites have large semimajor axes, orbiting at 35.7 and 69.5 Haumea radii ($R_{\rm H}$), where we use the volumetric Haumea radius of $R_{\rm H} \simeq 715$ km (from $495 \times 770 \times 960$ km estimated in Lockwood et al. 2014). The smaller inner satellite, Namaka, orbits with an eccentricity of 0.2 and an inclination of 13°. The larger outer satellite, Hi'iaka, has a less excited orbit, with an eccentricity of 0.05 and an inclination of ~2° (Ćuk et al. 2013). A deep search essentially ruled out additional regular satellites as small as $\sim 10^{-6}$ of Haumea's mass (Burkhart et al. 2016).

The larger satellite, Hi'iaka, orbits with a period of 49.462 ± 0.083 days (Ragozzine & Brown 2009). At this point in Hi'iaka's orbital evolution, it is expected to have been tidally despun and therefore rotating synchronously (or potentially in a higher-order spin–orbit resonance) with its orbital period. Assuming standard tidal theory, the large semimajor axis and low eccentricity of Hi'iaka would take much longer to achieve than despinning of a small satellite. In many tidal histories, the despinning of a small satellite is often considered to be effectively instantaneous due to the short timescales involved.

We present observations of Hi'iaka that clearly show that it is rotating ∼120 times faster than the expected synchronous spin period (Sections 2 and 3). Such a configuration is unusual for a regular satellite, as other regular satellites in the solar system are tidally despun, although it mirrors the recent discovery of rapidly rotating small moons of Pluto (Weaver et al. 2016). We then consider the implications for this rapid rotation in Section 4 by considering two end-member possibilities for Hi'iaka's formation: formation near the Roche limit of Haumea in a standard post-impact disk (Section 4.1) or formation near the present-day location (Section 4.2). This instigates an extensive discussion on the validity of using standard tidal "timescales" that suggests that initial conditions are very important, even for extensive tidal evolution, as demonstrated by numerical integration. We also consider the case of spin-up by a recent impactor (Section 4.3). We then draw conclusions and suggest future investigations in Section 5.

2. DATA

As the goal is to identify Hi'iaka's light-curve shape and period, only relative photometry is required. This simplifies the analysis considerably since our observations come from different telescopes under different observing conditions. Our primary data come from *Hubble Space Telescope* (*HST*) observations on 2009 February 4 and 2010 June 28 and Magellan observations on 2009 June 1.

The *HST* observations of the Haumea system comprised five *HST* orbits' worth of 100 s exposures of the Wide Field Planetary Camera 2 (Program 11971) and 10 *HST* orbits' worth of 44 s exposures of the Wide Field Camera 3 (Program 12243). Hereafter, we will refer to these as the "2009" and "2010" *HST* data, respectively. The 2009 observations were collected in an attempt to observe a possible mutual event between Hi'iaka and Namaka. They were well separated from Haumea, whose point-spread function (PSF) was removed. These satellites were too close to resolve at this epoch, so simple aperture photometry with a 4 pixel radius circular aperture was used to determine the light curve. We return to the implications for Namaka later, but for now we assume that the light curve is due entirely to Hi'iaka.

For the 2010 *HST* data, all three objects are resolved for the first four orbits. Triple PSF fits were performed as described in Ragozzine & Brown (2009) and Burkhart et al. (2016) to identify the exact locations of Haumea, Hi'iaka, and Namaka and to remove Haumea's PSF from the images. In the last six orbits, Namaka is too close to Haumea to resolve (these observations were chosen to capture a Haumea–Namaka mutual event, so this is unsurprising), and double PSF fits are used. In either case, Hi'iaka was far from Haumea and easily resolved. Simple aperture photometry was collected using a 4 pixel radius circular aperture, which is sufficient for our purposes. The PSF fits were designed for astrometry and do not return as reliable photometry. For more details on these observations see Burkhart et al. (2016). Several tests confirmed that the variability was real and centered on Hi'iaka. For example, investigation of the light curve of an identical aperture located opposite to Hi'iaka showed no significant variability. A few observations were significant outliers (due to cosmic-ray hits) and were removed from our data; contamination from cosmic rays was also the primary motivation of the choice of aperture size. Gaps due to Earth occultations are a larger concern, but do not preclude the 2010 data from showing a strong repeated variability, which we illustrate in Figure 1.

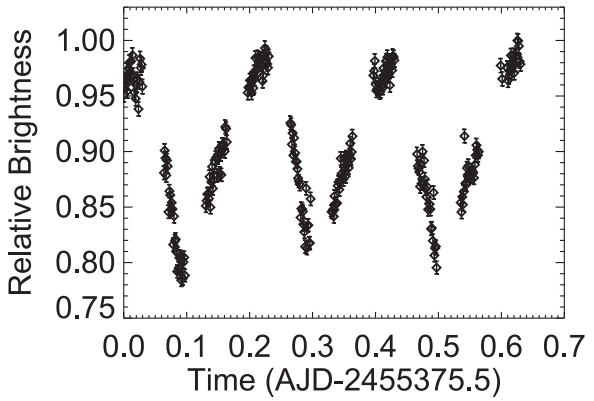

Figure 1. Unphased light curve for the 2010 *HST* data showing a strong repeated variability. These data only have Hi'iaka in the aperture. Investigations of other regions at the same Haumea-centric distance show no sign of variability. The error bars are estimated from photon noise. Gaps in the light curve are due to Earth occultations.

This system was also observed on the night of UT 2009 June 2 with the Magellan Baade telescope at Las Campanas Observatory in Chile. We used the Raymond and Beverly Sackler Magellan Instant Camera (MagIC). Observations were taken from the beginning of the night until it was unobservable, for a total of ∼5 hr. We centered the system on one of the four quadrants defined by the instrument's four amplifiers. The seeing was constant during the observations and consistently close to 0.″5, smaller than Hi'iaka's separation of 1.″4. The SITe CCD detector has a pixel scale of 0.″069 pixel^{-1}. We set the exposure times at 120 s to avoid saturation and optimize readout time. The filter selected was Johnson–Cousins *R*. Standard calibrations were taken at the beginning and end of the night. The telescope guiding system ensured that the pointing was constant to within an FWHM over the course of the observations.

Standard routines were used to trim, bias-subtract, and flat-field the images. Each exposure was then registered using the ISIS package (Alard 2000) to PSF match and subtract a template. The template image was the combination of the 20 sharpest images, using an average with sigma rejection on each pixel. Ordinary aperture photometry was then applied on the subtracted images to Haumea and two comparison stars of similar brightness in the field of view using the DAOPHOT II package (Stetson 1987, 1992). To remove the influence of Haumea on photometry at Hi'iaka's location, a two-dimensional Gaussian that was the best fit to Haumea was subtracted from the images.

For all of our observations, we can be confident that Hi'iaka's photometry was not affected by Haumea's variability

Table 1
Normalized Relative Photometry of Haumea

AJD (days)	Normalized Flux	Normalized Errors	Observing Program
2,454,867.136	0.9898	0.0103	1
2,454,867.138	0.9797	0.0102	1
2,454,867.157	0.9101	0.0099	1
2,454,867.159	0.9124	0.0099	1
2,454,867.161	0.9222	0.0099	1
2,454,867.163	0.9136	0.0099	1
2,454,867.203	0.8352	0.0095	1
2,454,867.205	0.8360	0.0095	1
2,454,867.207	0.8253	0.0094	1
2,454,867.209	0.8397	0.0095	1

Note. AJD is the HaumeA-centered Julian Date of the observations, after light-travel time corrections. The normalized flux and errors are derived from relative photometry measurements from (1) *HST* Program 11971 on 2009 February 4, (2) Magellan observations on 2009 June 1, and (3) *HST* Program 12243 on 2010 June 28. The photometry was normalized by dividing each individual data set by the maximum value of flux from that data set.

(This table is available in its entirety in machine-readable form.)

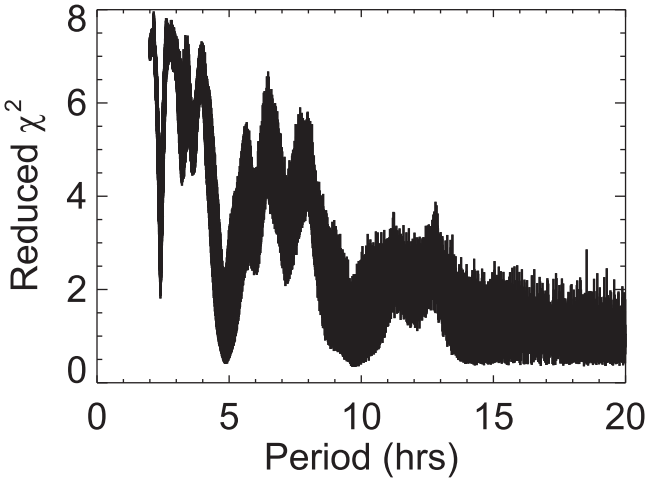

Figure 2. PDM periodogram for the Hi'iaka light-curve data. The minimum reduced χ^2 values correspond to the most likely rotation periods for Hi'iaka. The two regions of minima at 4.9 and 9.8 hr correspond to the single-peaked and double-peaked light curves, respectively. The double-peaked period has the lowest reduced χ^2 value and is preferred because Hi'iaka's significant variability is most likely due to the variable projected cross-sectional area of a rotating nonspherical body.

because we see no sign of Haumea's large-amplitude (∼25%) 3.9 hr rotational light curve. While it is possible that very minor contamination remains, it is far exceeded by the highly significant variations in Hi'iaka's light curve and does not affect our conclusions.

Each data set has been normalized to the respective maximum Hi'iaka brightness (all three go through a maximum), in order to provide relative photometry. We also investigated *HST* data from 2008 (Program 11518) and 2014–15 (Program 13873) with this rotation period. These data are composed of single-orbit investigations separated by weeks and have larger systematic errors, multiple filters, and much lower cadence (∼15 minutes). However, they showed the same types of trends as seen in the higher-cadence light curves: within an orbit, Hi'iaka's brightness could change by roughly ±10%. Other data sets are thus consistent with our conclusions.

Due to the different observation times, the Hi'iaka–observatory distance changes significantly, introducing light-travel time variations. Therefore, all times are converted to "HaumeA-centered Julian Date" (AJD), a clock local to the Haumea system and therefore mutually self-consistent. Table 1 presents this relative normalized photometry inferred from our observations.

3. ANALYSIS AND RESULTS

3.1. Period Analysis

The raw *HST* relative photometry given in Table 1 showed an extremely significant variability with a periodicity near 5 hr, and all three data sets indicated a similar sawtoothed shape. To identify a specific period, we employed phase dispersion minimization (PDM) using the IDL routine `PDM2` (M. Buie 2016, personal communication). PDM typically involves minimizing the dispersion of the data at a given phase (Stellingwerf 1978), but PDM2 seeks instead to minimize the reduced χ^2 statistic in order to determine the best period (Buie & Bus 1992). We searched periods from 2 to 20 hr to find a period that produced a self-consistent phased light curve. We note that the different observation geometries due to the heliocentric motion of Haumea and Earth (and any precession of Hi'iaka) only span ∼5° in viewing angle, so secular changes in Hi'iaka's light curve would be minimal and PDM remains an appropriate technique.

The resulting periodogram from PDM2 is shown in Figure 2. There are clearly two regions that are favored, with trial periods of ∼4.9 and ∼9.8 hr, which correspond to the single-peaked and double-peaked light curves, respectively. The rotation period would correspond to the single-peaked light curve if it were caused by albedo variegations, but this is atypical for objects the size of Hi'iaka. We therefore identify the 9.8 hr period as the rotation period of Hi'iaka, with the double-peaked light curve resulting from variable projected cross-sectional area of a rotating nonspherical body.

The trial periods with the lowest reduced χ^2 values were used to make a series of phase-folded plots. These were inspected by eye, as PDM2 only minimizes phase dispersion and does not invoke a smoothness criterion that is more consistent with a light curve. The phase-folded plot that was determined to be best is shown in Figure 3. This plot corresponds to the trial period with the second-lowest reduced χ^2 value (9.79736 hr), but was considerably smoother than the plot for the lowest value (9.71141 hr).

The PDM2 results show a forest of peaks corresponding to integer full rotations between our three disparate data sets. While additional work could potentially identify a more precise rotational period, this limited data set establishes that Hi'iaka has an unexpectedly rapid rotation rate that is ∼120 times faster than the 49.5-day orbital period.

3.2. Implications for Hi'iaka's Shape

From Figure 3, we can see that the brightness variation is 19% ± 1%, with a possible additional ∼1% systematic error due to our assumptions in producing the normalized relative photometry. The sawtooth shape indicates an irregularly shaped body, but without additional observations, we choose to approximate the shape of Hi'iaka as a triaxial ellipsoid with

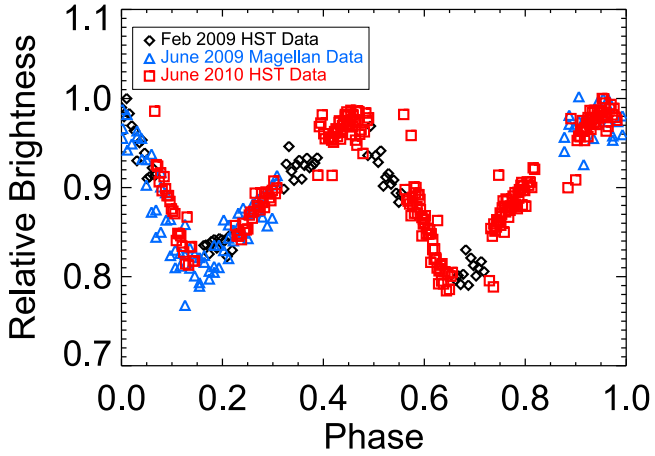

Figure 3. Phase-folded light curve for Hi'iaka relative normalized photometry. Black diamonds correspond to *HST* data from 2009 February 4 (Program 11971), blue triangles correspond to Magellan observations on 2009 June 1, and red squares correspond to *HST* data from 2010 June 28 (Program 12243). The data have been folded over a period of 9.79736 hr, but several plots with periods near 9.8 hr are similar. We conclude that the rotational period of Hi'iaka is approximately 9.8 hr with an amplitude of 19% ± 1%.

semiaxes $a > b > c$. The three (degenerate) parameters that control the light-curve amplitude of a triaxial ellipsoid are b/a, c/a, and θ, the angle between the line of sight and the rotational pole. The relationship between these parameters and the amplitude of the brightness variations in magnitudes (Δm) is (Benecchi & Sheppard 2013)

$$\Delta m = 2.5 \log \frac{a}{b} - 1.25 \log \left(\frac{a^2 \cos^2 \theta + c^2 \sin^2 \theta}{b^2 \cos^2 \theta + c^2 \sin^2 \theta} \right). \quad (1)$$

If Hi'iaka is nearly equator-on, then $\theta \approx 90°$, which gives a maximum value of b/a of approximately 0.81 for Hi'iaka. Another approximation to help break the degeneracy would be to limit b/a and c/a to values common for real solar system objects. We investigated Δm as a function of θ for objects presumed to be of similar size to Hi'iaka (150 km radius), using Equation (1). The objects considered were Eugenia, Psyche, Camilla, Eunomia, and Hyperion.[9] For these objects, θ between roughly 55° and 70° results in the brightness change observed in the Hi'iaka light curve ($\Delta m \simeq 0.23$). Hi'iaka has certainly experienced a different formation and evolution environment than these objects, but if it is roughly similar in shape, then this would imply that perhaps $\theta \approx 60°$ at the time of these observations.

3.3. Implications for Namaka's Light Curve

Recall that the 2009 observations actually contain both Hi'iaka and Namaka in our aperture. (They are unresolved as the purpose of these observations was to detect a satellite–satellite mutual event.) We assumed that variability was due to Hi'iaka, which we now revisit.

[9] These five objects were determined by investigating https://en.wikipedia.org/wiki/List_of_Solar_System_objects_by_size for objects with volumetric radii near 150 km. When performing calculations based on these bodies, we assume that they are represented by triaxial ellipsoids with parameters as listed on this Web page. Thisbe, Phoebe, and Hektor also had similar sizes, but their shapes are very inconsistent with the observed Hi'iaka light curve and are not used.

Due to the near commensurability between Hi'iaka's spin period and *HST*'s orbital period (seen in Figure 1 for the 2010 data) and an unfortunate phasing, the 2009 and 2010 data provide almost exclusive coverage of Hi'iaka's phase curve. Therefore, it is not possible to rigorously compare the 2009 mutual event data with the "true" Hi'iaka light curve inferred from light curves at other epochs. The light curve is reasonably smooth, but this is partly by construction. Therefore, it is difficult to say for certain what effect Namaka's light curve or the possible mutual event had on the photometry.

Even if Namaka's light curve is entirely constant over this time interval, it would create a ∼20% dilution of Hi'iaka's light curve, even in normalized photometry. This may be visible in Figure 3 near a phase of 0.2, where the 2009 February data are systematically brighter than the 2009 June Magellan data. Near 0.7 in phase, perhaps the true light curve of Hi'iaka is deeper than portrayed. In any case, the shape and structure of the light curve are preserved, and our inference of a rotational period of 9.8 hr for Hi'iaka is not affected.

Inspection of Figure 3 suggests that major variability on short timescales beyond Hi'iaka's light curve is unlikely. Namaka is ∼4 times fainter than Hi'iaka in this filter, so a lack of variability at the ∼5% level would suggest that Namaka is not more than ∼20% variable. Given Namaka's size, it is likely to be aspherical like Hi'iaka (or more so). So, an apparent lack of Namaka's light curve would suggest either a slow rotation (much longer than 10 hr) or a face-on orientation (which would require significant obliquity, since Namaka's orbit is very nearly edge-on). We note that Namaka has not shown significant variability in other single-orbit *HST* data. The 2010 data were obtained near a Haumea–Namaka mutual event, and no robust variability is detected, but Namaka is close to or within Haumea's PSF, so this does not provide a strong constraint. Altogether, the data hint that Namaka's spin period is longer than roughly a day. Whether or not the data indicate a slowly rotating Namaka, it is worth noting that for orbital periods longer than ∼1 day, Namaka's high eccentricity would likely result in a chaotic rotation due to spin–orbit resonance overlap (Dobrovolskis 1995; Murray & Dermott 2000).

A Hi'iaka-Namaka mutual event (shadowing and/or occultation) would last up to 100 minutes and could result in a ∼25% drop in flux. An event this strong is not detected. Grazing events that are shorter than about 30 minutes would be too weak to detect. In between is a wide range of possibilities, but the combined light curve does not seem to contain any obvious mutual event. This does not entirely rule out a mutual event as it could have occurred during Earth occultation. The lack of a mutual event has weak implications for the possible orbits of Hi'iaka and Namaka, which are beyond the scope of this work.

3.4. Implications for Haumea System Photometry

Haumea has been the subject of significant photometric study, often without resolving Hi'iaka. Since Hi'iaka is ∼5% as bright as Haumea and has a ∼20% light curve, failing to account for Hi'iaka in unresolved photometry can introduce a ∼1% error in understanding Haumea. As Haumea has a ∼25% intrinsic variability (Rabinowitz et al. 2008), Hi'iaka's effect will only be important for precise measurements.

Reviewing the observations for Haumea's "Dark Red Spot" (Lacerda et al. 2008; Lacerda 2009), we do not believe that Hi'iaka's light curve has any effect on these conclusions, which

are spread over multiple nights (and therefore would average out Hi'iaka's effect) and stronger than 1%.

On the other hand, Ragozzine & Brown (2009) predicted that Haumea and Namaka would undergo mutual events, and several ground-based measurements were obtained by multiple teams. These mutual events are only a few percent in amplitude, and Hi'iaka's light curve did provide some confusion. With the phase curve provided in Figure 3, it should be possible to minimize the confusion from Hi'iaka's orbit, although this requires fitting Hi'iaka's spin phase until future work identifies Hi'iaka's spin period and phase more precisely.

3.5. Precession of Spin Axis

The process of satellite despinning is directly connected to the evolution of satellite obliquity (the angle between the satellite's spin vector and the primary-satellite orbit vector). As Hi'iaka is rapidly rotating, there is a chance that it has retained a significant obliquity. Indeed, Pluto's small satellites have very high obliquities (90°–120°; Weaver et al. 2016), and a measurement of Hi'iaka's obliquity will similarly provide information on the formation and evolution of its spin. Hi'iaka's obliquity cannot be discerned in a single epoch, but Haumea's mass will cause Hi'iaka's spin vector to precess, which would manifest itself as changes in the light-curve shape over time.

Without information about the shape and obliquity of Hi'iaka, we seek here to provide only an approximate sense of how precession affects the spin axis direction. We average over the "fast angles" that describe Hi'iaka's spin and orbital orientation and assume a circular orbit for simplicity. In this case, the obliquity (ϕ) remains constant and the precessing angle is known as the equinox. The precession period is given by

$$P_{\rm Precession} = -\frac{2}{3}\frac{P_{\rm orb}^2}{P_{\rm spin}}\frac{C}{C-A}\frac{1}{\cos\phi}, \quad (2)$$

where C and A are the standard moments of inertia ($C > B > A$) and the spin, orbital, and equinox precession periods are labeled (e.g., Stacey & Davis 2008). For a triaxial ellipsoid of uniform density, the moments of inertia are

$$A = \frac{M}{5}(b^2 + c^2) \quad (3)$$

$$C = \frac{M}{5}(a^2 + b^2). \quad (4)$$

Since $C/(C-A)$ for Hi'iaka is unknown, the median value of the previously mentioned Hi'iaka-sized objects (2.34) is used for illustration.

The minimal precession period occurs when the obliquity is zero ($\phi = 0$, i.e., alignment of the spin and orbit axes), which gives $P_{\rm Precession} \simeq 26$ yr. This first-order estimate indicates that Hi'iaka's spin precession could be visible within only a few years, as only a fraction of the precession cycle is required to provide observable changes in the light curve.

Larger obliquities produce larger light-curve changes, but also have slower precession periods. To illustrate this, we assume a simple linear precession of the equinoxes and calculate θ (the angle between the line of sight and Hi'iaka's spin axis) as a function of time. Without a more sophisticated model, we approximate Hi'iaka's orbit as fixed at epoch HJD 2,454,615.0 (Ragozzine & Brown 2009) and do not include small ($\lesssim 3°$) changes in the orbital viewing angle.

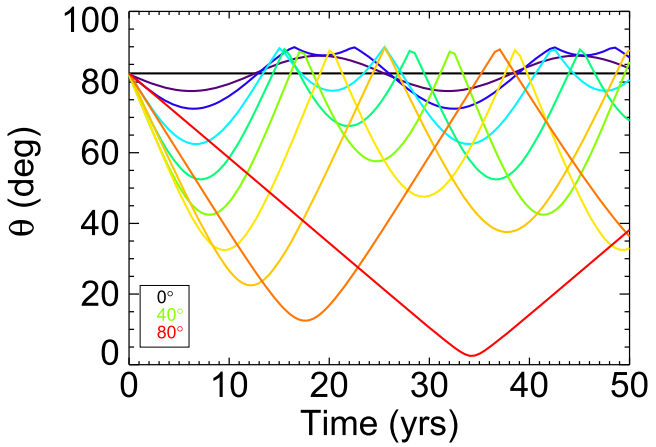

Figure 4. Plot of the angle between the Earth line of sight and the spin axis direction (θ) over 50 yr. Each line is a different obliquity (ϕ), starting at 0° (black horizontal line; no precession), followed by 5° (purple) and then 10° (dark blue). The obliquity is then incremented by 10° until 80° (red). The y-axis ranges from $\theta = 0°$ (sub-Earth point at Hi'iaka's pole) to $\theta = 90°$ (sub-Earth point on Hi'iaka's equator), where values larger than 90° are "reflected" since the effect on the light-curve amplitude (Equation (1)) is symmetric. As shown in Equation (2), larger obliquities are associated with longer precession periods. The light-curve amplitude of Hi'iaka suggests the present value of θ around 60°, with values less than 45° unlikely. For clarity, the precessing equinox angle starts at the same value for each curve, but in actuality, the present-day Hi'iaka could be anywhere in the precession cycle. Therefore, we cannot rule out any particular obliquity.

The results, which are only illustrative, are shown in Figure 4. For an obliquity of zero, Hi'iaka's spin is nearly equator-on (since the orbit is nearly edge-on at the fixed epoch). Increased obliquity leads to more pronounced changes, but also slower evolution, in accordance with Equation (2).

Based on our earlier sense from the shapes of Hi'iaka-sized objects, a present-day value of $\theta \approx 60°$ would require an obliquity of $\gtrsim 20°$. Such a configuration suggests a precession rate of a few degrees per year. Zero obliquity is only possible if Hi'iaka is more spherical than other objects of similar size. By investigating objects with the full range of plausible shapes, only the most extreme objects could have $\theta \lesssim 45°$ at the present epoch. This does not rule out any particular obliquity, since we do not know the phase of the equinox precession cycle.

We find no significant evidence in our observations of a change in amplitude in the light curve due to the precession of the spin axis, but we present this as something to look for in future observations of the Haumea system. In the triaxial approximation using shapes from objects similar in size to Hi'iaka, the light-curve amplitude can change by ~0.01 mag per degree of change in θ. Combined with a precession rate ranging from 1° to 10° per year and the fact that our observations are from ~7 yr old data, if Hi'iaka has a significant obliquity, it seems very likely that the light curve would be detectably different in new observations. New observations can confirm precession, but uniquely solving for the shape and obliquity of Hi'iaka would likely require sampling the light curve at multiple distinct epochs. In particular, the sawtooth shape of Hi'iaka's light curve (Figure 3) indicates that a triaxial ellipsoid is not a perfect model and Hi'iaka may be more angular.

Our precession timescale estimates are sensitive to poorly known shape parameters, so the timescales could easily vary by tens of percent from what has been presented here. Still, observations of Hi'iaka spread over ∼10 yr should be able to put valuable constraints on Hi'iaka's obliquity.

For comparison, we also calculated the precession periods of the small moons of Pluto using Equation (2), using dimensions and obliquity values assuming triaxial ellipsoids with the parameters from Weaver et al. (2016). This yields precession periods of approximately 23, 3.0, 5.6, and 31 yr for Styx, Nix, Kerberos, and Hydra, respectively, though there is some uncertainty. The effect of Charon complicates their spin dynamics (Correia et al. 2015; Showalter & Hamilton 2015), but hopefully long-term observations can provide information on these moons as well.

4. FORMATION HYPOTHESES

The newfound result that Hi'iaka has a rapid rotation rate and potentially a significant obliquity helps provide insight into the formation and evolution of this moon, the Haumea system, and the Haumea collisional family, which we now explore in detail.

Hi'iaka is orbiting in a low-eccentricity, low-inclination orbit at ∼70 primary radii, which, combined with Namaka's similar orbital state, cannot be explained through known capture mechanisms (Ragozzine & Brown 2009). Thus, Hi'iaka formed around Haumea. There are two major end-member explanations for its present dynamical state: (1) Hi'iaka mostly formed near the Roche limit and dynamically evolved outward to its present location, or (2) Hi'iaka mostly formed near/at its present location.

At first glance, neither of these mechanisms is fully satisfying, even before considering the origin of Hi'iaka's rapid rotation. Some theories for the formation of the Moon include additional satellites (e.g., Canup et al. 1999), potentially long-lived (e.g., Stacey & Davis 2008), and Haumea's satellites are in a broadly similar regime. However, dynamical evolution to its present location through tides seems to require extreme tidal parameters for Haumea. Using the volumetric radius, estimated physical parameters, and standard tidal equations requires unreasonable tidal parameters (Ćuk et al. 2013). Recent work by Quillen et al. (2016) shows that including the nonspherical nature of Haumea only gives a factor of 2 boost to the tidal evolution, overturning the argument of Ragozzine & Brown (2009) that this might be important. Although these first-order estimates fall far short, Quillen et al. (2016) admit that additional analysis and an improved understanding of Haumea's size (which is still unknown), shape, and geophysical parameters may allow for such extensive tides to move from unrealistic to plausible. Even if strong tides can be invoked, for some values of the masses of the satellites, the inability to maintain dynamical stability between interacting satellites with such significant tidal interactions is another major drawback to this hypothesis (Ćuk et al. 2013).

Formation at the present location avoids issues with tides, but prompts the question of why the proto-satellite disk extended to such a large semimajor axis, well beyond the regular satellite region of known bodies. Interactions with other objects (including Namaka) or the proto-satellite disk could have pushed Hi'iaka outward. In the case of Pluto, collisional expansion of the disk (or of multiple generations of satellites) can cause significant semimajor axis evolution (Bromley & Kenyon 2015; Walsh & Levison 2015). These simulations included massive Charon, which is presumably a key component of the formation of Pluto's small moons, so these results are likely not relevant to the Haumea system. The most plausible hypothesis for such an extended disk around Haumea is that it formed subsequent to a collision onto a previous satellite (called the ur-satellite) of Haumea (Schlichting & Sari 2009). Ćuk et al. (2013) explore this hypothesis in detail and find that it is mostly plausible. Further work is required to explain why this disk results in two widely separated moons (at ∼35 and ∼70 primary radii), though once near this configuration, Ćuk et al. (2013) suggest that resonant dynamics and standard tidal evolution can potentially reproduce the present eccentricities and inclinations. A downside to this hypothesis is that it removes any connection between the unusually rapid rotation of Haumea (caused by the initial impact) and the formation of a tight dynamical family, as the latter is independent of the former. Leinhardt et al. (2010) point out that smoothed particle hydrodynamics simulations cannot reproduce the creation of a rapidly spinning primary and a relatively large ur-satellite, which suggests that this model may not be entirely self-consistent. Alternatively, since the formation of Haumea and the ur-satellite can occur early in the outer solar system when collisions are common, perhaps there are a reasonable set of collisions that form the ur-satellite and then spin up Haumea (without destroying the binary). Even if forming a rapidly rotating Haumea and an ur-satellite is reasonably probable, this formation hypothesis proposes that the spin-up event is effectively independent of the ur-satellite collision that forms the family. The combination of these two low-probability events seems unreasonably low (Campo-Bagatin et al. 2016); it is not clear why the only detectable collisional family in the Kuiper Belt would happen to form around the fastest-spinning large body in the solar system.

A full examination of these formation hypotheses is beyond the scope of this work, but we do investigate how Hi'iaka's rapid spin would fit into both of these end-member models.

4.1. Formation Close to Haumea and Evolved Out

If Hi'iaka forms close to Haumea (near the Roche limit) and then evolves out, an initial expectation is that despinning tides would have slowed its rapid rotation early in its history when it was much closer to Haumea.

The effect of despinning tides on Haumea can be parameterized in many ways. New models that explicitly include the expected frequency dependence of tides have been applied to some spin–orbit problems (e.g., Efroimsky & Williams 2009; Makarov & Efroimsky 2014; Ferraz-Mello 2015). Many second-order effects could be important, such as solar interactions (e.g., Porter & Grundy 2012), interactions with the other satellite[10] (Ćuk et al. 2013), spin–orbit resonances and chaos (e.g., Wisdom et al. 1984; Dobrovolskis 1995), and other potential issues. To simplify the problem into a tractable one and for comparison to previous

[10] It is worth noting that the tidal dynamics of the Haumea system are unique among objects in the solar system. It has large dynamically interacting satellites like the giant planet satellite systems, but these evolve very slowly in semimajor axis due to weak tidal dissipation in gas and ice giants ($Q \gtrsim 10^4$). Among terrestrial/icy primaries with large dissipation, Haumea is unique in having two known moons that are both relatively massive and strongly interacting.

work, we begin by using a simplified technique that can identify important dynamical results to approximately first order. Hence, we elect to use the "classic" constant Q models of Goldreich & Peale (1968), keeping in mind that they are, at best, just approximations to a more complex history.

In these models, the rate of change of the spin frequency ω is given by

$$\dot{\omega} = \mathrm{sign}(\omega - n)\frac{3}{2}\frac{k_{2s}}{Q_s}\frac{1}{C_s}\left(\frac{M_p}{m_s}\right)\left(\frac{r_s}{a}\right)^3\frac{GM_p}{a^3} \quad (5)$$

where n is the mean motion, k_2 is the second-order tidal Love number, Q is the tidal quality factor, M and m are masses, r is the radius, a is the semimajor axis, and G is the gravitational constant. In our case, the primary ("p") is Haumea and the secondary ("s") is Hi'iaka.

4.1.1. Initial Rough Quantitative Estimates

In order to provide very rough quantitative estimates for the evolution of the Haumea–Hi'iaka system, we follow the method of Murray & Dermott (2000) for estimating k_2 (see also Quillen et al. 2016):

$$k_2 = \frac{3}{2(1 + \mu_{\mathrm{eff}})} \quad (6)$$

where μ_{eff} is the effective rigidity given by

$$\mu_{\mathrm{eff}} = \frac{19\mu}{2\rho g r} \quad (7)$$

where $\mu = 4 \times 10^9$ N m^{-2} is the assumed rigidity for an icy body, ρ is the density, r is the radius, and g is the surface gravity. We take μ from Murray & Dermott (2000); however, the appropriate rigidity for tidal analyses could easily be off by orders of magnitude.

After assuming a value for the classic tidal dissipation parameter Q and implicitly choosing a frequency dependence and rheology for the body (Efroimsky & Williams 2009), we can arrive at the classic estimate for the tidal despinning timescale:

$$\tau_\omega = \frac{\omega}{\dot{\omega}} \approx \frac{2}{15\pi}\frac{Q_s}{k_{2s}}\left(\frac{\rho_s}{\rho_p}\right)^{3/2}\left(\frac{a}{R_p}\right)^{9/2}P_{\mathrm{orb}}. \quad (8)$$

Similar calculations result in the timescale for changes in the orbital frequency n:

$$\tau_n = -\frac{2}{3}\tau_a = -\frac{2}{18\pi}\frac{Q_p}{k_{2p}}\frac{M_p}{m_s}\left(\frac{a}{R_p}\right)^5 P_{\mathrm{orb}} \quad (9)$$

where M_p is the mass of Haumea and m_s is the mass of Hi'iaka.

We find below that calling these "timescales" is inappropriate. However, starting with these equations results in estimates for tidal properties and timescales shown in Table 2. This initial rough analysis indicates that Hi'iaka's despinning timescale is longer than the age of the solar system. However, this conclusion requires many simplifying assumptions, which we now explore in greater detail.

4.1.2. Time-evolved Numerical Solution

The standard equation for the despinning "timescale" (τ_ω) evaluated at the present location of Hi'iaka is a poor approximation of whether Hi'iaka could have despun. Under the assumption of active tidal evolution, the semimajor axis of the satellite has changed significantly. As the despinning tides are strongly dependent on a ($\tau_\omega \propto a^6$), τ_ω is certain to be an overestimate of the time required to despin a satellite. Furthermore, the initial spin period (which nominally determines the number of despinning timescales required for synchronization) is not known and could cover quite a range.

To explore the actual tidal evolution, we developed a simple numerical model that calculates the time evolution of the spin frequency during semimajor axis expansion. We continue to make the assumption of a simplified tidal model, no spin–orbit resonances or chaos, and neglecting outside influences (e.g., Namaka).

Equation (9) implies that the semimajor axis evolution has the form $a(t) = (a_f - a_0)(t/T)^{2/13} + a_0$, where T is assumed to be the age of the solar system,[11] a_0 is the initial semimajor axis, and a_f is the present semimajor axis.

At every time step, the appropriate value of a was then used to determine how the rate of change of the spin frequency, $\dot{\omega}$, changes with time. The spin is evolved following Euler's method: $\omega(t_i) = \omega_0 + \Delta t\dot{\omega}(t_{i-1})$, where ω_0 is the initial spin frequency, i is the iteration number, Δt is the time step, and $\dot{\omega}(t_{i-1})$ is the rate of change of the spin frequency for the previous iteration, calculated from Equation (5). In order to resolve the evolution, which is orders of magnitude more rapid at the beginning of the simulation, we use exponentially increasing values of Δt so that the iteration time steps t_i are evenly spaced logarithmically. We checked many different values for the number of iterations, and there were no issues with convergence. Under certain assumptions (always supersynchronous or subsynchronous, always reaching a_f at time T, and retaining a_0 and ω_0), the evolution equations can be solved for analytically, and these results exactly confirmed the numerical simulations.

Our nominal runs used the parameters given in Table 2 and $Q_s = 100$. Multiple a_0 and ω_0 values were tested, and the results of one of these tests, with $a_0 = 2000$ km (just outside Haumea's Roche limit), are shown in Figure 5. It is clear that the initial spin period is an important variable in determining whether or not Hi'iaka would be synchronous at the present time. Simulations with other values of a_0 are similar, but they demonstrate that a_0 is also an important variable.

We investigated whether it was possible to determine analytically the time needed to despin given actual semimajor axis evolution and retaining a_0 and ω_0 in the solution (even though common practice is to neglect these). The result is a quartic polynomial in the despinning time to the $1/13$ power with no path to a general solution. Furthermore, the analytical results were nearly as time-consuming to calculate as simply propagating the motion numerically. Hence, the numerical technique is preferred.

For understanding how Hi'iaka's rapid spin rate affects our understanding of its formation, time evolution assuming certain parameters is only a first step. The more relevant question is, for what tidal parameters (e.g., k_{2s}/Q_s) does Hi'iaka despin in the age of the solar system, as a function of the initial semimajor axis and spin period? We combined our numerical technique with a bisection search in order to answer this

[11] In this hypothesis, where Hi'iaka is coeval with the Haumea family, we rely on the results of Ragozzine & Brown (2009) and Volk & Malhotra (2012) that the family is ancient with an age comparable to the age of the solar system.

Table 2
Key Parameters for Planetary Satellites

Object	Satellite	Mass (kg)	Radius[a] (km)	Density (kg m^{-3})	a (km)	P_{orb} (days)	P_{spin} (days)	k_2[b]	g (m s^{-2})	τ_ω[c] (yr)	References
Haumea	⋯	4.006×10^{21}	715	2600	⋯	⋯	⋯	0.03	0.3	⋯	1, 2
Haumea	Hi'iaka	2×10^{19}	150	1000	49880	49.462	0.408	0.0004	0.06	2×10^{10}	1, 3
Haumea	Namaka	2×10^{18}	75	1000	25657	18.2783	⋯	0.00007	0.02	2×10^{9}	1, 3
Pluto	⋯	1.304×10^{22}	1187	1860	⋯	⋯	⋯	0.05	0.6	⋯	4
Pluto	Charon	1.59×10^{21}	606	1700	17540	6.3872	6.3872	0.01	0.3	9×10^{5}	4
Pluto	Styx	1.0×10^{15}	5.2	1700	42656	20.1616	3.24	0.0000009	0.002	3×10^{12}	5, 6
Pluto	Nix	5.1×10^{16}	19	1700	48694	24.8546	1.829	0.00001	0.009	4×10^{11}	5, 6
Pluto	Kerberos	1.5×10^{15}	6.0	1700	57783	32.1676	5.31	0.000001	0.003	1×10^{13}	5, 6
Pluto	Hydra	6.5×10^{16}	21	1700	64738	38.2018	0.4295	0.00001	0.01	2×10^{12}	5, 6
Earth	⋯	5.9722×10^{24}	6371	5515	⋯	⋯	⋯	1	9.8	⋯	7
Earth	Moon	7.3459×10^{22}	1738	3341	384400	27.322	27.322	0.3	2	5×10^{7}	7
Eris	⋯	1.66×10^{22}	1163	2500	⋯	⋯	⋯	0.09	0.8	⋯	8, 9
Eris	Dysnomia	2×10^{20}	342	1000	37350	15.774	⋯	0.001	0.1	2×10^{8}	8, 10
Makemake	⋯	4.4×10^{21}	715	2300	⋯	⋯	⋯	0.04	0.6	⋯	11
Makemake	MK2 (4%)	2.8×10^{18}	87.5	1000	21000	12.4	⋯	0.00008	0.02	2×10^{9}	12

Notes. Key parameters and results from tidal despinning calculations.
[a] Radii for Haumea and the small satellites of Pluto are the volumetric radii, calculated using $R = \sqrt[3]{abc}$.
[b] Value of k_2 calculated using Equation (6).
[c] Despinning timescale in the current position of each satellite, calculated using Equation (8) and $Q = 100$.
References. (1) Ragozzine & Brown 2009; (2) Lockwood et al. 2014; (3) Ćuk et al. 2013; (4) Stern et al. 2015; (5) Showalter & Hamilton 2015; (6) Weaver et al. 2016; (7) Stacey & Davis 2008; (8) Brown & Schaller 2007; (9) Sicardy 2011; (10) Santos-Sanz et al. 2012; (11) Brown 2013; (12) Parker et al. 2016.

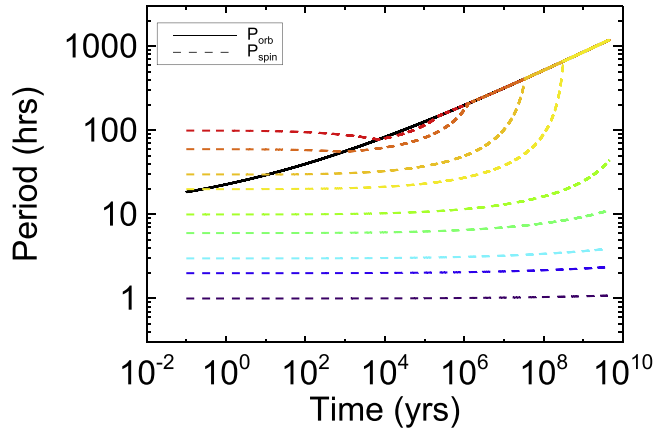

Figure 5. Results of the time-evolved tidal despinning for Hi'iaka. Physical and tidal parameters from Table 2 were assumed, along with an initial semimajor axis of $a_0 = 2000$ km. Nine initial spin periods were tested (dashed lines) and compared to the evolution of the orbital period of Hi'iaka (solid line). Analytical solutions (not shown for clarity) match exactly those models. According to this tidal model, it is only possible for Hi'iaka to despin for longer initial spin periods. For initial spin periods comparable to the current value, the despinning cannot keep up with the orbital period and Hi'iaka never despins. A more detailed picture of the tidal parameters needed to despin Hi'iaka is shown in Figure 6.

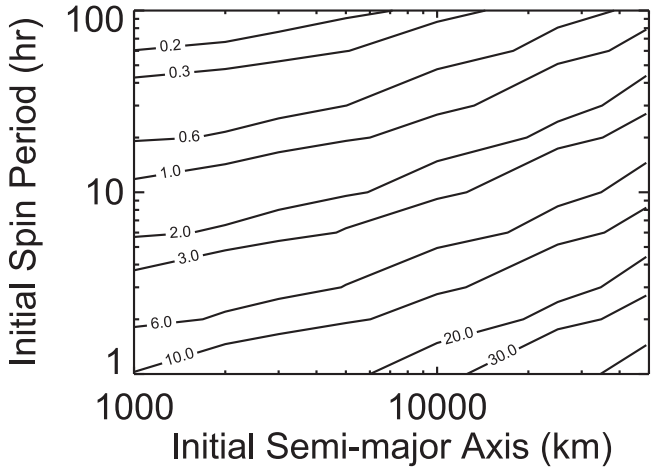

Figure 6. Contour plot of Z, the scale factor by which the nominal $\frac{k_{2s}}{Q_s} = 4 \times 10^{-6}$ must be multiplied in order for Hi'iaka to despin after ~4.5 Gyr under our assumed tidal model. We find that the initial semimajor axis and initial spin period are important, with an approximate relation of $Z \propto a_0 \omega_0$. Uncertainty in tidal parameters allows for a wide range of plausible Z values, making Hi'iaka's evolution unclear. If despinning tides are 100 times stronger than this estimate, then Hi'iaka can despin for any initial conditions, including formation at its present location. If tidal despinning tides are 10 times weaker than the nominal estimate, then Hi'iaka would not despin for any initial conditions, including significant tidal evolution.

question. Specifically, we calculate the value of Z, such that $\frac{k_{2s}}{Q_s} = Z\frac{0.0004}{100}$ leads to despinning within a few percent of the age of the solar system, where the numerical values are the nominal values listed in Table 2.[12] The semimajor axis evolution of Hi'iaka starts at a_0 and ends at the present position in the age of the solar system, as before.

[12] Equivalently, Z could modify the unknown physical parameters, such as the radius of Hi'iaka.

Slight changes in the parameters (a_0, w_0, and Z) led to very large differences in the time needed to reach synchronous. This sensitivity is due to the strong dependence on semimajor axis, which is evolving rapidly. This is reflected in Figure 5 by the sharp downturns in the computed spin evolution (even on a log–log plot). If synchroneity is just missed at an early epoch, then it can take a very long time to "catch up."

We show the value of Z in a contour plot in Figure 6. Despite the strong dependence on parameters, Z is approximately proportional to $a_0 w_0$. This is consistent with an analytical investigation of the dependence of Z on these parameters. We have included $a_0 \simeq a_f$ as a prelude to the discussion below where Hi'iaka does not undergo tidal evolution.

As the actual effective tidal parameters of Hi'iaka are uncertain by orders of magnitude, Z is highly uncertain as well. These results show that if $\frac{k_{2s}}{Q_s}$ is 100 times larger than the nominal value, then Hi'iaka will despin in practically any circumstance (no tidal evolution and initial very rapid rotation). If $\frac{k_{2s}}{Q_s}$ is 10 times smaller than nominal, then Hi'iaka would not despin in the age of the solar system, even if it started interior to the Roche lobe with a very slow spin rate. The wide variation in outcomes based on a relatively small uncertainty in tidal parameters is frustrating, but these results clearly indicate that Hi'iaka need not tidally despin.

That a highly tidally evolved regular satellite could avoid despinning seemed contrary to our initial understanding. The common assumption for regular satellites is that, since the despinning timescale at the Roche limit is so small, the satellites quickly synchronize. And, once in a synchronous state, only "small" corrections are needed to maintain synchroneity as the satellite evolves outward due to tides. A separation of timescales between the satellite synchronization and longer-term evolution of the semimajor axis is then invoked (e.g., Gladman et al. 1996; Goldreich & Sari 2009). Thus, such satellites are expected to be synchronous, even if the despinning timescale at the present position is longer than the age of the system.

We have identified significant issues with this common story. In particular, satellites of terrestrial planets experience significant tidal evolution (since Q_p is so small, compared to gas giants). It is therefore plausible that semimajor axis evolution (or, more precisely, the evolution of the mean motion) is so fast that despinning tides simply cannot keep up. If satellite tides are weak enough compared to primary tides, there must be a regime where despinning cannot keep up with orbital expansion and the satellite does not remain synchronous. This is an arguable proposition even if our models for tides are incorrect compared to newer models based on appropriate geophysics. While our estimates of time-averaged approximate tidal parameters and corresponding timescales may be off by orders of magnitude, it remains the case that supersynchronous regular satellites like Hi'iaka could be explained by despinning rates that are slower than semimajor axis expansion.

As an example of how despinning tides could be weak, we consider the recent analysis by Efroimsky (2015), which proposes that the tidal dissipation rate of small bodies is controlled by viscosity (η), not strength (μ). Using $\eta \approx 10^{15}$ Pa for warm ice (Ojakangas & Stevenson 1989), which is probably a strong (1–5 orders of magnitude) underestimate for the viscosity of Hi'iaka/Namaka, we find that Equation (65) in Efroimsky (2015) shows that the dissipation rate k_2/Q in these small bodies is in the regime where it is proportional to $1/(\eta\chi)$, where χ is related to the spin or orbital frequencies ($\simeq 10^{-4}$). Using a quadrupole approximation ($l = 2$) and values from Table 2 suggests that the effective k_{2s}/Q_s in this geophysical model is 4×10^{-6}. This is 100 times weaker than our estimates based on the classical rigidity model above and would prevent Hi'iaka from despinning under any reasonable initial condition. Considering that cold[13] ice would have a much higher viscosity, the effective k_{2s}/Q_s could potentially be as low as 10^{-9}! These geophysical arguments would be sufficient to weaken tidal despinning of Hi'iaka to the point where it cannot keep up with synchronous and would maintain any rapid initial spin.

Another issue with the common story is the assumption that satellites quickly despin since their despinning timescales are so short (e.g., due to formation near the Roche limit). This can ignore the also rapid semimajor axis evolution; if the despinning timescale changes from 100 yr to 1000 yr due to semimajor axis expansion that happens in 50 yr, then synchroneity is not an inevitable outcome. Furthermore, the "despinning timescale" at any semimajor axis is not an effective way to estimate whether a satellite is despun, since it ignores the major influence of a_0 and w_0. Numerical simulations are more self-consistent.

The idea that the satellite nearly instantly evolves to a synchronous state also oversimplifies the effects of spin–orbit resonances and associated chaos. It is likely that small regular satellites experience chaotic spin evolution due to overlapping spin–orbit resonances as long as the spin period is within a factor of several times the (changing) orbital period (Wisdom et al. 1984; Dobrovolskis 1995; Murray & Dermott 2000). While Hi'iaka is spinning much too fast for chaos now, when the orbital period was tens of hours, it could have been in the chaotic regime and therefore not seriously affected by despinning tides. For despinning tides to succeed as satellites slow down, they must be able to pass through this chaotic barrier. Our results in Figures 5 and 6 suggest that if Hi'iaka *ever* reaches a spin period as rapid as ~10 hr, then despinning tides would not succeed at synchronization (with the nominal tidal parameters). A chaotic regime early in its evolution could have readily imparted such a rapid spin state.

Together, these results suggest that the common assumptions that imply inevitable synchronization of regular satellites do not hold up to more detailed investigation. In particular, Hi'iaka's rapid spin (either 9.8 or 4.9 hr) is not inconsistent with formation near the Roche limit followed by semimajor axis expansion to its present location.

4.1.3. Comparison to Other Systems

One way of roughly validating our understanding of despinning is to check whether our model would match observations in other systems. For comparison, the numerical solutions described in Section 4.1.2 were also tested on Namaka and the Earth–Moon system using the parameters given in Table 2. Though these methods do not include spin–orbit resonance or chaos and require major assumptions about tidal properties, the results of these tests are consistent with observations. The results for the other systems listed below follow from Table 2 and Equation (8).

1. The Moon and Charon are able to despin, as expected.
2. Namaka despins for reasonable initial spin periods (all tested initial periods except for 1 hr).
3. Styx, Nix, Kerberos, and Hydra do not despin in the age of the solar system.
4. Dysnomia has likely despun.

[13] At present, the tidal dissipation in Hi'iaka is approximately 1 W for the whole body, indicating that tidal heating is not a significant source of heat; in a body so small, retained primordial heat would be minimal.

5. Makemake's recently discovered moon, MK2, has likely despun.

We note that the classification as "despun" really means that the current rotation rate is within the regime where low-order spin–orbit resonances are important. Understanding whether the moons reside in a resonance (not necessarily synchronous) or a regime afflicted by spin–orbit chaos will require additional observational and theoretical investigation. Furthermore, this assumes the nominal tidal parameters; as we saw for Hi'iaka, changes within the orders-of-magnitude uncertainty can lead to substantially different outcomes.

Since the small satellites of Pluto are known to be supersynchronous like Hi'iaka, we discuss their results briefly here. The formation of these moons is not well understood. Although matching detailed simulations is problematic (e.g., Lithwick & Wu 2008), the near-resonant locations suggest that these moons may have been pushed outward during Charon's orbital evolution (e.g., Ward & Canup 2006). As Charon is much larger than these moons, it evolves much more quickly, potentially reaching its current position in only ∼10 Myr (Dobrovolskis et al. 1997, p. 159; Cheng et al. 2014). Resonant expansion with Charon would have resulted in rapid semimajor axis expansion for these moons, orders of magnitude faster than their expected despinning timescales. As with Hi'iaka, even if these moons used to be much closer to Pluto, their semimajor axis expansion could have been so rapid as to stifle tidal despinning, leaving them with their observed rapid rotation rates and high obliquities.

4.1.4. Conclusions for the Tidal Evolution Hypothesis

A detailed investigation into the tidal despinning hypothesis shows that regular satellites need not despin if they had moderately rapid initial spin rates and despinning tides that are weaker than rapid semimajor axis expansion. For reasonable parameters and classic tidal models, this is fully consistent with the rapid spin states observed for Hi'iaka and Pluto's moons. Hence, the supersynchronous rotation rate for Hi'iaka does not suggest that Hi'iaka was never close to Haumea. Hi'iaka's spin rate does not weigh against the hypothesis that Haumea's satellites formed close to Haumea and experienced significant tidal expansion.

Similar processes that control the spin rate of Hi'iaka also affect its obliquity on comparable timescales. Obliquities are also affected by the final tail of collisional formation and complex dynamics, such as Cassini states (e.g., Fabrycky et al. 2007). Hence, we expect the same results to hold for Hi'iaka's obliquity: tides may not have affected it, even if it formed very near to Haumea. Whether, and how, Hi'iaka's obliquity affects our understanding of how it formed is beyond the scope of this work.

We note that the standard models for eccentricity tides have similar dependencies on semimajor axes to despinning tides. Therefore, the importance of including semimajor axis evolution is also applicable to eccentricity tides. One additional complication is that both the primary and secondary contribute to eccentricity tides and often in opposite ways, as discussed by Ćuk et al. (2013). Depending on the tidal model, rapidly rotating Hi'iaka could actually result in eccentricity pumping even by the secondary (e.g., Mignard 1980). Most of the concerns expressed above about inappropriate assumptions for despinning tides apply similarly to eccentricity tides. Yet, in most models, satellite despinning should occur more rapidly than satellite circularization. The rapidly rotating Hi'iaka then could be strong evidence that Hi'iaka's eccentricity was not lowered due to satellite tides. As with the spin rate, resonances —this time mean motion resonances with Namaka—preclude us from drawing conclusions about the initial state of Hi'iaka's orbit, as discussed extensively in Ćuk et al. (2013).

4.2. Formation Far Out

In the hypothesis where Hi'iaka forms near its present location, different considerations are needed to understand its current spin state. Figure 6 shows that, if Hi'iaka was always near its present location, it would only despin if the initial rotation period was long ($\gtrsim$100 hr) or the tidal parameters several times larger than the nominal value. Hi'iaka's current spin period could be comparable to its spin period after formation far from Haumea. In this sense, it is similar to irregular satellites that are also unlikely to despin (Melnikov & Shevchenko 2010).

Unfortunately, there is little detail about what we might expect for the initial spin period of Hi'iaka in the hypothesis where Hi'iaka forms far from Haumea. As the inclination of Hi'iaka, Namaka, and Haumea's equator are all highly consistent, this requires formation in a proto-satellite disk with damped inclinations and eccentricities (Schlichting & Sari 2009; Ćuk et al. 2013). An impact with an ur-satellite that creates Hi'iaka, Namaka, and the collisional family would initially create a huge cloud of debris that then participates in a collisional cascade that creates the low-inclination disk. At the frigid temperatures of the Kuiper Belt, the coagulation into satellites should follow entirely gas-free solid-body formation by accretion. In this case, the spin and obliquity of the final Hi'iaka are controlled by the last few stochastic collisions (see also Section 4.3.2). This suggests that the initial spin period and obliquity cannot be reasonably inferred. In particular, Hi'iaka's rapid spin is also consistent with the hypothesis that it formed near its present location.

It is important to recognize that we have considered the end-member possibilities; a case where the satellites form far from the Roche limit but also experience significant semimajor axis evolution is also possible. In any of these models, despinning tides might somewhat slow an initially more rapid spin to the present 9.8 hr period.

4.3. Other Possible Spin-up Explanations

As shown in Figure 6, if despinning tides are ∼100 times stronger than the nominal estimate given in Table 2, then both formation hypotheses may predict a near-synchronous rotation rate for Hi'iaka. Given the orders-of-magnitude uncertainty in tidal parameters, we also briefly consider other possible explanations for recently spinning up Hi'iaka.

Based on Hi'iaka's physical and orbital properties, we can immediately rule out gravitational effects from the Sun (except perhaps as would be relevant for Cassini states), as well as radiation effects like Yarkovsky and YORP. Namaka is too small and too far away to exert a significant influence, except to contribute mildly to spin–orbit chaos.

Haumea has the largest quadrupole moment of objects of its size and a rapid rotation rate. Hence, it is a candidate for

considering whether some kind of spin–spin resonance was important (Batygin & Morbidelli 2015; Showalter & Hamilton 2015). However, even in this extreme case, it seems unlikely that spin–spin resonances are a dominant effect on Hi'iaka (Batygin & Morbidelli 2015). This is emphasized by the fact that Hi'iaka's spin period is 9.8 hr compared to Haumea's 3.9 hr. While potentially close to the 5:2 spin–spin resonance, it is very unlikely that there is an important dynamical influence from this weak resonance, particularly at the present distance of 70 primary radii. The apparent resonance could easily be due to the fact that any two periods will be coincidentally somewhat near some ratio of small integers. Future work that identifies a more precise spin rate of Hi'iaka can compare it to the known precise spin rate of Haumea (Lockwood et al. 2014) to be sure.

Another potential explanation for Hi'iaka's spin rate is a recent collision. Even if tides had despun Hi'iaka to a synchronous rotation rate, a collision can potentially reset the spin. The collision only needs to be as "recent" as a few despinning timescales at the present location of Hi'iaka (measured in Gyr, but with significant uncertainty). Pluto's satellites (Weaver et al. 2016) show impact craters, and certainly Hi'iaka is also subject to collisions.

We do not consider explicitly the probability of any particular collision, but focus instead on identifying what kind of collisions are even plausible with the observed properties of Hi'iaka. The collision must provide a significant spin-up without destroying Hi'iaka or significantly perturbing its near-circular orbit, which would gain a much higher eccentricity than observed (0.05) with a velocity change of only $\sim 10\,\mathrm{m\,s^{-1}}$. It turns out that this limits the range of plausible impactors, even when considering simple conservation of momentum and angular momentum.

We considered several types of collisions that had a possibility of spinning Hi'iaka to its currently observed rotational rate. The two possible options were a small heliocentric impactor and a Haumea-centric satellite (now part of Hi'iaka). We considered two different scenarios for each case. For each scenario we created a simulation in MATLAB using Monte Carlo methods. A given simulation would randomly determine a number of parameters within reasonable ranges and, using conservation of linear and angular momentum, determine the result of a collision on Hi'iaka's spin and eccentricity. These simulations ignore a large host of known physical and geophysical effects of impacts, but their only goal is to identify whether there are any collisions that can possibly conserve momentum and angular momentum, spin up Hi'iaka, and leave it on a nearly circular orbit.

4.3.1. Heliocentric Impactors

The heliocentric impactor case was tested using a "bullet" impactor with a mass between 10^{14} and 10^{16} kg, 0.001% to 0.1% the mass of Hi'iaka. This impactor collided with a velocity between 300 and $2500\,\mathrm{m\,s^{-1}}$, consistent with heliocentric impactors given Haumea's orbit. The first heliocentric scenario tested involved a cratering impact in which a uniform cone of material was ejected perpendicular from the impact direction (which may not be perpendicular to the surface of Hi'iaka). We found that in collisions that resulted in a rotational period of less than 10 hr, the impactor was capable of imparting velocity changes of well over $1000\,\mathrm{m\,s^{-1}}$, and it was impossible to impart any velocity kicks of less than $100\,\mathrm{m\,s^{-1}}$. This magnitude of a velocity change would drastically change the orbit of Hi'iaka (orbiting at $\sim 75\,\mathrm{m\,s^{-1}}$), effectively ruling out this scenario.

The second heliocentric scenario involved one of the same impactors hitting with a very high impact parameter in a hit-and-run-type collision, in which the impactor rebounds perpendicular to the impact location and continues on with some fraction of its original speed, imparting both a linear and angular kick to Hi'iaka. This type of collision was able to impart the observed spin rate with linear kicks of less than $10\,\mathrm{m\,s^{-1}}$. However, these results were contingent on an impactor just barely clipping the surface of Hi'iaka and bouncing off at the same very low angle, usually leaving with only one-quarter of its initial velocity. This type of collision is unlikely, and physically the bounce is improbable, so we conclude that this type of collision most likely was not the cause of Hi'iaka's present state.

Although not surprising, we feel that these results are sufficient to rule out heliocentric impactors as origins for Hi'iaka's spin.

4.3.2. Haumea System Impactors

We also consider the possibility that Haumea had three satellites, one of which collided with Hi'iaka to spin it up. For the Haumea-centric impactor case, we considered two smaller satellites moving at lower speeds, with relative velocities at infinite separation ranging from zero (co-orbital) to $300\,\mathrm{m\,s^{-1}}$. We first considered a merging event of the two small satellites. For purposes of modeling how the angular momentum is related to the final spin, the satellites were modeled as spheres, and the merging simply as the two spheres sticking together. The merging simulations were able to generate rapid spins while imparting linear kicks of less than $10\,\mathrm{m\,s^{-1}}$, which would preserve Hi'iaka's eccentricity.

The final scenario involved a Haumea satellite, proto-Hi'iaka, more than half the mass of today's Hi'iaka, being struck by a smaller satellite, a rubble pile, a loose collection of rock and ice held together by its own gravity. In this scenario, the smaller impactor collides with proto-Hi'iaka with some impact parameter, resulting in a shear in which part of the impactor is removed, joining proto-Hi'iaka, while the rest continues on unaffected. This simulation also yielded positive results, with a wealth of collisions that imparted the necessary spin with low linear kicks.

While we did not evaluate the probability of Haumea-centric impactors yielding the present-day Hi'iaka, the wide ranges of acceptable impacts suggest that this is a possible mechanism, though much more detailed simulations would be necessary to truly assess their plausibility. So, another hypothesis for Hi'iaka's spin is that it was despun, but a third satellite recently (within $\sim \tau_\omega$) collided with Hi'iaka to produce the observed spin. Given that the other hypotheses can also reproduce Hi'iaka's spin, Occam's razor would suggest that we need not invoke a previous third satellite.

These results also confirm that, wherever Hi'iaka formed, impacts with other Haumea-centric bodies in the formation disk could have readily provided a rapid spin while preserving its low eccentricity and inclination.

5. CONCLUSION

In summary, our work has led to the following conclusions:

1. Observations show that Hi'iaka has a clear light curve with a sawtooth shape and amplitude of 19% ± 1%. The three data sets with sufficient information are consistent with a double-peaked rotation period of about 9.8 hr. Thus, Hi'iaka is rotating ~120 times faster than its orbital period.
2. Hi'iaka may also have a significant obliquity that would be imminently detectable as changes in light-curve shape.
3. Despinning tides do not necessarily produce synchronous regular satellites. The time needed to despin a satellite depends on the initial semimajor axis and rotation rate. Considering likely initial spin rates and rapid semimajor axis expansion allows for Hi'iaka to maintain its highly supersynchrnous rotation, even if it formed near the Roche limit for nominal tidal parameters. Therefore, Hi'iaka's spin rate does not rule out significant tidal evolution.
4. Hi'iaka's spin rate is also consistent with a formation near its present location.
5. Heliocentric impactors cannot spin up Hi'iaka without destroying it or severely affecting its orbit. However, Haumea-centric impactors can readily provide the observed spin.

Unfortunately, Hi'iaka's spin does not provide a strong discriminator between different formation hypotheses, particularly given the large uncertainty in possible tidal parameters. Thus, we suggest that future work to identify better and more self-consistent models for the formation of the Haumea system and family should primarily focus on explaining other observations.

We thank Marc Buie for sharing his IDL library, including the `PDM2` code that was used in this work. D.R. acknowledges discussions with Matija Ćuk and others concerning possible explanations for Hi'iaka's unexpectedly rapid spin rate. We wish to thank the anonymous reviewers for their comments and suggestions, which improved the quality of this paper.

Support was provided by NASA through grant HST-GO-13873 from the Space Telescope Science Institute (STScI), which is operated by the Association of Universities for Research in Astronomy, Inc., under NASA contract NAS 5-26555.

Software: ISIS (Alard 2000), DAOPHOT II (Stetson 1987, 1992), PDM2 (M. Buie 2016, personal communication).

REFERENCES

Alard, C. 2000, A&AS, 144, 363
Batygin, K., & Morbidelli, A. 2015, ApJ, 810, 110
Benecchi, S. D., & Sheppard, S. S. 2013, AJ, 145, 124
Bromley, B. C., & Kenyon, S. J. 2015, ApJ, 809, 88
Brown, M. E. 2013, ApJL, 767, L7
Brown, M. E., Barkume, K. M., Ragozzine, D., & Schaller, E. L. 2007, Natur, 446, 294
Brown, M. E., & Schaller, E. L. 2007, Sci, 316, 1585
Brown, M. E., Schaller, E. L., & Fraser, W. C. 2012, AJ, 143, 146
Buie, M. W., & Bus, S. J. 1992, Icar, 100, 288
Burkhart, L. D., Ragozzine, D., & Brown, M. E. 2016, AJ, 151, 162
Campo-Bagatin, A., Benavidez, P. G., Ortiz, J. L., & Gil-Hutton, R. 2016, MNRAS, 461, 2060
Canup, R. M., Levison, H. F., & Stewart, G. R. 1999, AJ, 117, 603
Carry, B., Snodgrass, C., Lacerda, P., Hainaut, O., & Dumas, C. 2012, A&A, 544, A137
Cheng, W. H., Lee, M. H., & Peale, S. J. 2014, Icar, 233, 242
Correia, A. C. M., Leleu, A., & Robutel, P. 2015, arXiv:1506.06733
Ćuk, M., Ragozzine, D., & Nesvorný, D. 2013, AJ, 146, 89
Dobrovolskis, A. R. 1995, Icar, 118, 181
Dobrovolskis, A. R., Peale, S. J., & Harris, A. W. 1997, Dynamics of the Pluto-Charon Binary (Pluto and Charon) (Tucson, AZ: Univ. Arizona Press)
Efroimsky, M. 2015, AJ, 150, 98
Efroimsky, M. 2015, AJ, 151, 130
Efroimsky, M., & Williams, J. G. 2009, CeMDA, 104, 257
Elliot, J. L., Person, M. J., Zuluaga, C. A., et al. 2010, Natur, 465, 897
Fabrycky, D. C., Johnson, E. T., & Goodman, J. 2007, ApJ, 665, 754
Ferraz-Mello, S. 2015, CeMDA, 122, 359
Gladman, B., Quinn, D. D., Nicholson, P., & Rand, R. 1996, Icar, 122, 166
Goldreich, P., & Peale, S. J. 1968, ARA&A, 6, 287
Goldreich, P., & Sari, R. 2009, ApJ, 691, 54
Lacerda, P. 2009, AJ, 137, 3404
Lacerda, P., Jewitt, D., & Peixinho, N. 2008, AJ, 135, 1749
Leinhardt, Z. M., Marcus, R. A., & Stewart, S. T. 2010, ApJ, 714, 1789
Levison, H. F., Morbidelli, A., Vokrouhlický, D., & Bottke, W. F. 2008, AJ, 136, 1079
Lithwick, Y., & Wu, Y. 2008, arXiv:0802.2951
Lockwood, A. C., Brown, M. E., & Stansberry, J. 2014, EM&P, 111, 127
Lykawka, P. S., Horner, J., Mukai, T., & Nakamura, A. M. 2012, MNRAS, 421, 1331
Makarov, V. V., & Efroimsky, M. 2014, ApJ, 795, 7
Marcus, R. A., Ragozzine, D., Murray-Clay, R. A., & Holman, M. J. 2011, ApJ, 733, 40
Melnikov, A. V., & Shevchenko, I. I. 2010, Icar, 209, 786
Mignard, F. 1980, M&P, 23, 185
Murray, C. D., & Dermott, S. F. 2000, Solar System Dynamics (Cambridge: Cambridge Univ. Press)
Ojakangas, G. W., & Stevenson, D. J. 1989, Icar, 81, 220
Ortiz, J. L., Thirouin, A., Campo Bagatin, A., et al. 2012, MNRAS, 419, 2315
Parker, A. H., Buie, M. W., Grundy, W. M., & Noll, K. S. 2016, arXiv:1604.07461
Porter, S. B., & Grundy, W. M. 2012, Icar, 220, 947
Quillen, A. C., Kueter-Young, A., Frouard, J., & Ragozzine, D. 2016, arXiv:1607.08591
Rabinowitz, D. L., Barkume, K., Brown, M. E., et al. 2006, ApJ, 639, 1238
Rabinowitz, D. L., Schaefer, B. E., Schaefer, M., & Tourtellotte, S. W. 2008, AJ, 136, 1502
Ragozzine, D., & Brown, M. E. 2009, AJ, 137, 4766
Santos-Sanz, P., Lellouch, E., Fornasier, S., et al. 2012, A&A, 541, A92
Schaller, E. L., & Brown, M. E. 2008, ApJL, 684, L107
Schlichting, H. E., & Sari, R. 2009, ApJ, 700, 1242
Showalter, M. R., & Hamilton, D. P. 2015, Natur, 522, 45
Sicardy, B., Ortiz, J. L., Assafin, M., et al. 2011, Natur, 478, 493
Stacey, F. D., & Davis, P. M. 2008, Physics of the Earth (Cambridge: Cambridge Univ. Press)
Stellingwerf, R. F. 1978, ApJ, 224, 953
Stern, S. A., Bagenal, F., Ennico, K., et al. 2015, Sci, 350, 1815
Stetson, P. B. 1987, PASP, 99, 191
Stetson, P. B. 1992, in ASP Conf. Ser. 25, Astronomical Data Analysis Software and Systems I, ed. D. M. Worrall, C. Biemesderfer, & J. Barnes (San Francisco, CA: ASP), 297
Thirouin, A., Sheppard, S. S., Noll, K. S., et al. 2016, arXiv:1603.04406
Trujillo, C. A., Sheppard, S. S., & Schaller, E. L. 2011, ApJ, 730, 105
Volk, K., & Malhotra, R. 2012, Icar, 221, 106
Walsh, K. J., & Levison, H. F. 2015, AJ, 150, 11
Ward, W. R., & Canup, R. M. 2006, Sci, 313, 1107
Weaver, H. A., Buie, M. W., Buratti, B. J., et al. 2016, Sci, 351, e0030
Wisdom, J., Peale, S. J., & Mignard, F. 1984, Icar, 58, 137